

## QUANTUM-MECHANICAL STUDY OF INTERNAL STRUCTURAL TRANSFORMATIONS IN Pb-SUPERSATURATED Pb-Sn ALLOYS

<sup>1</sup>Martin FRIÁK, <sup>1,2</sup>Petr ČÍPEK, <sup>2</sup>Jana PAVLŮ, <sup>1,3</sup>Pavla ROUPCOVÁ, <sup>1</sup>Ivana MIHÁLIKOVÁ,  
<sup>4</sup>Šárka MSALLAMOVIČ, <sup>4</sup>Alena MICHALCOVÁ

<sup>1</sup>*Institute of Physics of Materials, v.v.i., Czech Academy of Sciences, Brno, Czech Republic, EU,  
[friak@ipm.cz](mailto:friak@ipm.cz), [500008@mail.muni.cz](mailto:500008@mail.muni.cz); [roupcova@ipm.cz](mailto:roupcova@ipm.cz); [mihalikova@ipm.cz](mailto:mihalikova@ipm.cz);*

<sup>2</sup>*Department of Chemistry, Faculty of Science, Masaryk University, Brno, Czech Republic; EU,  
[houserova@chemi.muni.cz](mailto:houserova@chemi.muni.cz)*

<sup>3</sup>*Central European Institute of Technology (CEITEC), Brno University of Technology, Brno, Czech  
Republic, EU*

<sup>4</sup>*Department of Metals and Corrosion Engineering, University of Chemistry and Technology in Prague,  
Prague, Czech Republic, EU, [Sarka.Msallamova@vscht.cz](mailto:Sarka.Msallamova@vscht.cz), [Alena.Michalcova@vscht.cz](mailto:Alena.Michalcova@vscht.cz)*

<https://doi.org/10.37904/nanocon.2023.4749>

### Abstract

Motivated by a decades-long controversy related to the crystal structure of Pb-supersaturated solid solutions of Pb in Sn, we have performed a quantum-mechanical study of these materials. Focusing on both body-centred-tetragonal  $\beta$ -Sn and simple-hexagonal  $\gamma$ -Sn structures, we have computed properties of two alloys with the chemical composition  $\text{Pb}_5\text{Sn}_{11}$ , i.e. 31.25 at. % Pb, which is close to the composition of the experimentally found alloy (30 at. % Pb). The 16-atom computational supercells were designed as multiples of the elemental  $\beta$ - and  $\gamma$ -Sn unit cells, where the Pb atoms were distributed according to the special quasi-random structure (SQS) concept. Full structural relaxations of both  $\beta$ - and  $\gamma$ -phase-based alloys resulted in very significant re-arrangements into structures which do not exhibit any apparent structural features typical for the original alloys, and are, therefore, difficult to classify. The formation energies of the  $\beta$ - and  $\gamma$ -phase-originating equilibrium phases are 50 meV/atom and 53 meV/atom, respectively. Therefore, they are not stable with respect to the decomposition into the elemental lead and tin. Moreover, our calculations of elastic constants of both phases revealed that they are close to mechanical instability. Our results indicate that the studied Pb-supersaturated Pb-Sn solid solutions may be prone to structural instability, transformations into different phases and decomposition. Our findings may contribute into the identification of the reason why the subsequent experimental studies did not reproduce the initial published data.

**Keywords:** Pb-Sn alloys, stability, supersaturation, quantum-mechanical calculations

### 1. INTRODUCTION

The tin-rich Sn-Pb alloys have been used for centuries for numerous products, such as organ pipes [1] or jewellery. More recent industrial applications are represented by, for example, food cans as well as a broad range of electrical-engineering products containing Pb-Sn solders. While currently banned due to their Pb content [2], Pb-Sn alloys are still important when addressing the issue of millions of tons of electrical-engineering waste.

An original motivation for our study was a decades-long controversy associated with the crystal structure of Pb-supersaturated solid solutions of Pb in Sn. This fundamental basic-science issue is crucial for non-equilibrium states in Pb-supersaturated Pb-Sn alloys when decomposing into Pb-rich and Sn-rich phases [3]. The decomposition is the consequence of a low solubility of lead in tin. In particular, the solubility is negligible

in the low-temperature  $\alpha$ -Sn, see **Figure 1(a,b)**, and only up to 1.3 at. % [3] in the room-temperature tetragonal body-centred  $\beta$ -phase, see **Figure 1(c)**, exhibiting also a strong dependence on the temperature [4,5]. Regarding the atomic-scale decomposition processes, they are active at room temperature as well as at yet lower temperatures because the melting temperature of tin is relatively low.

The above-mentioned controversy is related to a few older experimental papers reporting the existence of (i) a simple-hexagonal (so-called  $\gamma$ -phase) Sn-rich Pb-Sn alloys with Pb concentration as high as 26 at. %, see, e.g., Ref. [6], which was not found in subsequent studies [7], or (ii) a Pb-supersaturated  $\beta$ -phase Pb-Sn alloys with the Pb concentrations within a range of 5-30 at. % Pb, see Ref. [8]. We made several attempts to synthesize these Pb-supersaturated alloys of Sn following the steps, which were published in Ref. [3], but neither the  $\gamma$ -phase nor  $\beta$ -phase Pb-supersaturated Pb-Sn alloys were obtained. Therefore, we have applied theoretical (quantum-mechanical) methods to shed light on the stability of Pb-supersaturated Pb-Sn alloys.

## 2. COMPUTATIONAL METHODOLOGY

Our quantum-mechanical calculations were performed employing the Vienna Ab initio Simulation package (VASP) [9,10] within the density functional theory (DFT) [11,12] using projector augmented wave (PAW) [13,14] pseudopotentials (in particular, Ni\_pv, Mn\_pv and Sn\_d versions from the potpaw\_PBE.52 VASP database). The exchange-correlation energy was parametrized within the generalized gradient approximation (GGA) by Perdew, Burke and Ernzerhof (PBE'96) [15]. The plane-wave energy cut-off was set to 500 eV. We applied the Methfessel-Paxton smearing scheme of order 1 with the smearing parameter set to 0.1.

## 3. RESULTS

Building upon our previous results related to properties of the  $\alpha$ - and  $\beta$ -phase Sn [16], we have newly studied structural, elastic and thermodynamic properties of two polymorphic variants of the Pb-supersaturated Pb-Sn alloys; one based on the  $\beta$ - and the other on the  $\gamma$ -phase of Sn. As the authors of Ref. [8] reported Pb concentrations as high as 30 at. %, we employed 16-atom supercells (see below) with five Pb atoms inside, i.e. the Pb concentration of 31.25 at. %.

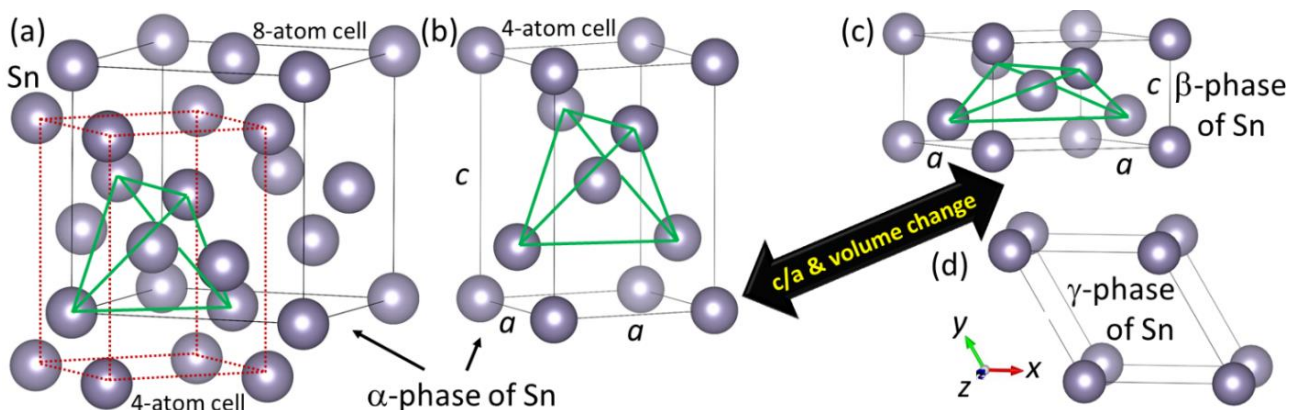


**Figure 1** Simplified visualizations of computational cells used in our study: (a) the  $\alpha$ -phase Sn modelled as an 8-atom diamond-structure cell, which can be described as well by a 4-atom body-centred tetragonal cell (see the red dotted lines), (b) the smaller 4-atom cell of the  $\alpha$ -Sn, (c) the  $\beta$ -phase (which can be obtained by changes of the  $c/a$  ratio and volume from the cell shown in part (b)), and finally (d) the 1-atom simple hexagonal unit cell of the  $\gamma$ -Sn. Note that some atoms are shown together with their periodic images. The tetrahedral structural unit is marked by green lines and shows the internal distribution of atoms.

The computed concentration is as close to 30 at. % reported in Ref. [8] as is possible employing the 16-atom supercell. The Pb atoms were distributed according to the special quasi-random structure (SQS) approach

[17]. The SQS supercells are designed to optimally model an ideally disordered solid solution under constraints imposed by the periodically repeated supercells. The SQS supercells were generated by the Universal Structure Predictor: Evolutionary Xtallography (USPEX) software package [18-20]. The 16-atom computational cell of the  $\beta$ -phase was initially designed as a  $1 \times 2 \times 2$  multiple of the 4-atom cell shown in **Figure 1(c)**, and the 16-atom cell of the  $\gamma$ -phase was initially designed as a  $4 \times 2 \times 2$  multiple of the 1-atom cell shown in **Figure 1(d)**.

We focused on the structural instabilities of some of the Pb-supersaturated Pb-Sn alloys. As the first example, we have performed structural relaxations in  $\text{Pb}_5\text{Sn}_{11}$  solid solution of the  $\beta$ -phase type modelled by a 16-atom supercell with a random distribution of Pb atoms. The computational cell, see **Figures 2(a,b)**, underwent a full relaxation when the internal atomic positions as well as the computational cell shape and volume were changed to minimize the energy. During the process of energy minimization, the components of the stress tensor as well as the forces acting upon atoms were significantly reduced, too, as the former are responsible for cell shape changes while the latter for the internal re-arrangement of atoms. Importantly, a significant internal restructuring has occurred, as visible in the comparison of **Figures 2(a,b)** with **Figures 2(c,d)**. The final structure in **Figures 2(c,d)** is difficult to crystallographically categorize as it does not have typical structural characteristics of any of the common Sn phases ( $\alpha$ ,  $\beta$  or  $\gamma$ ), and the distribution of Pb and Sn atoms is also lowering the symmetry as another factor complicating the analysis.

In order to address the thermodynamic stability of the studied phases, we evaluated their formation energy  $\Delta E_f$ . Its mathematical expression for a general  $\text{Pb}_x\text{Sn}_y$  binary alloy is as follows:

$$\Delta E_f(\text{Pb}_x\text{Sn}_y) = \frac{E(\text{Pb}_x\text{Sn}_y) - x * E(\text{Pb}) - y * E(\text{Sn})}{x + y},$$

where we used the static-lattice energy  $E(\text{Pb}_x\text{Sn}_y)$  of the  $\text{Pb}_x\text{Sn}_y$  alloy and energies of constituting pure elements in their ground-state structures, in particular,  $E(\text{Pb})$  for the face-centred-cubic (fcc) Pb and  $E(\text{Sn})$  for the diamond-structure  $\alpha$ -Sn. The computed formation energy is equal to 0.050 meV/atom.

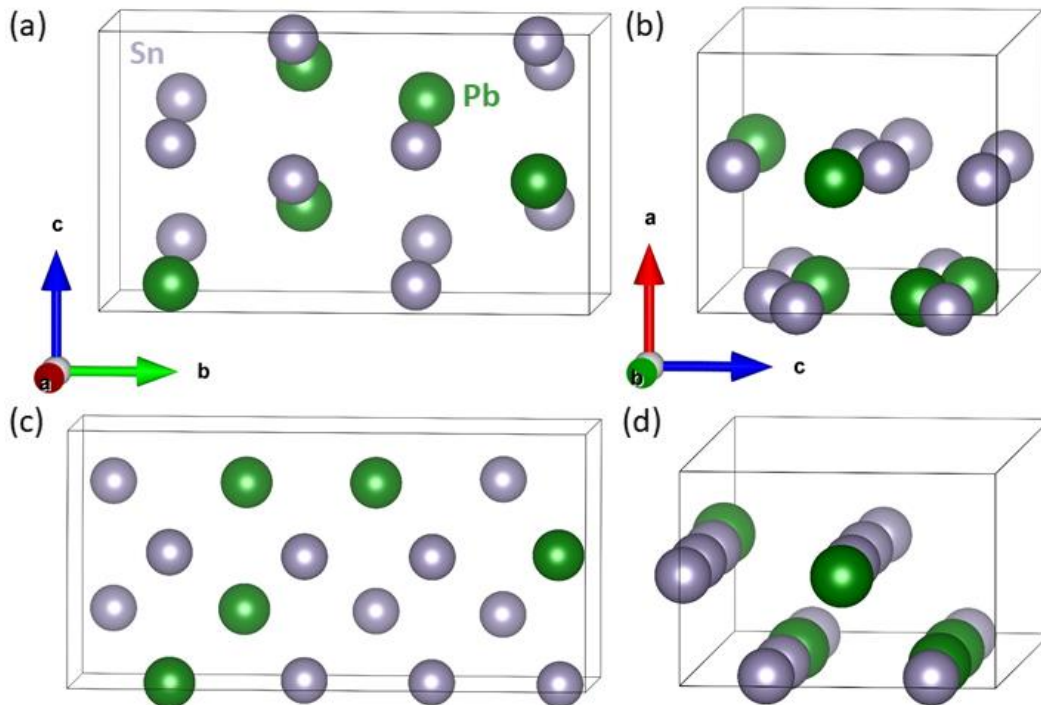


**Figure 2** The  $\beta$ -phase-based  $\text{Pb}_5\text{Sn}_{11}$  solid solution modelled by a 16-atom supercell: (a,b) initial structure, (c,d) strongly re-arranged structure due to the energy minimization process. The grey (green) spheres correspond to Sn (Pb) atoms.

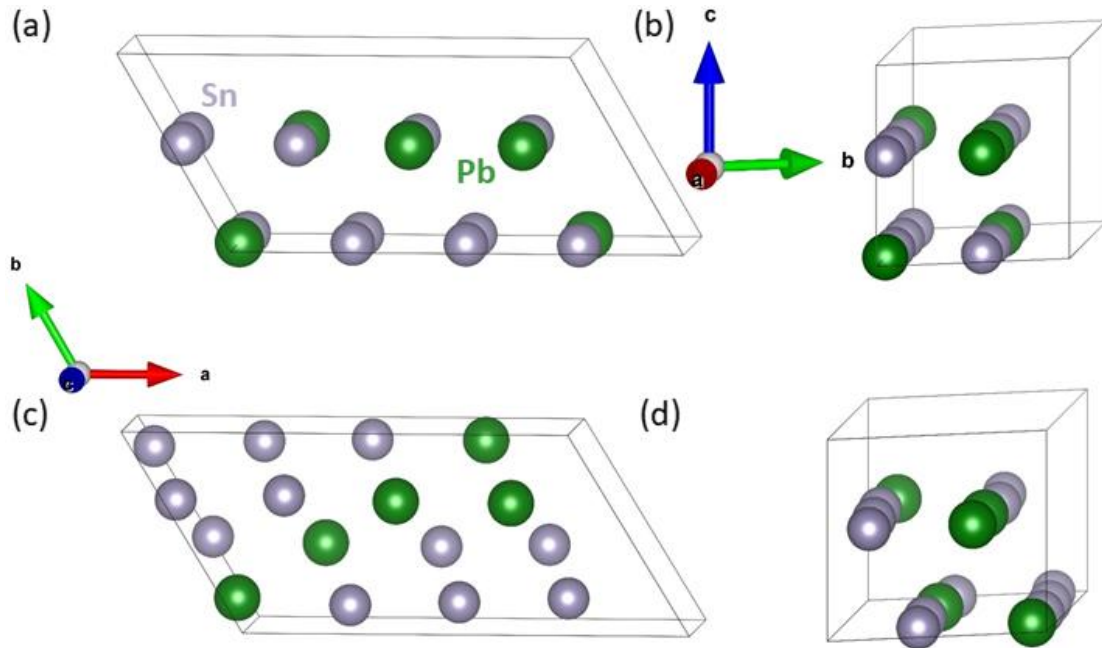


**Figure 3** The  $\gamma$ -phase-based  $Pb_5Sn_{11}$  solid solution modelled by a 16-atom supercell: (a,b) initial structure, (c,d) strongly re-arranged structure due to the energy minimization process. The gray (green) spheres correspond to Sn (Pb) atoms.

Another example of very significant internal relaxations is the  **$Pb_5Sn_{11}$  solid solution of the  $\gamma$ -phase type**. Here, the original supercell, see **Figures 3(a,b)**, contained again 16 atoms, and the full relaxation resulted in another phase, see **Figures 3(c,d)**, which is again very difficult to identify.

The computed formation energy is equal to and 0.053 meV/atom. Therefore, this structure, as well as the previous one, is unstable regarding the decomposition into the elemental end-members, lead and tin.

In order to examine the mechanical stability and elastic properties of both studied polymorphs, we have determined a full tensor of their elastic constants using the stress-strain method [21], and we present the computed elastic constants (in GPa) as 6×6 matrices including their eigenvalues:

Elastic constants of the phase in **Figures 2(c,d)**:

46	43	39	0	0	0
43	58	30	0	0	-1
39	30	57	0	-1	-1
0	0	0	5	0	0
0	0	-1	0	18	0
0	-1	-1	0	0	17

Eigenvalues: 4, 5, 17, 18, 28, 129 (in GPa)

Elastic constants of the phase in **Figures 3(c,d)**:

64	40	21	-1	-1	3
40	62	31	0	0	0
21	31	72	1	2	-8
-1	0	1	9	-3	-1
-1	0	2	-3	5	0
3	0	-8	-1	0	13

Eigenvalues: 3, 10, 12, 21, 51, 128 (in GPa)

An expected error-bar of our calculated elastic constants is a few GPa, and all eigenvalues of the elastic stiffness matrices are positive for both studied states. However, the lowest eigenvalues are very close to zero, indicating that both systems are very close to mechanical instability, as a system is mechanically stable if all eigenvalues of the 6×6 matrix of elastic constants are positive.

The directional dependencies of single-crystal Young's moduli of the analysed phases are shown in **Figure 4** and they exhibit a very strong elastic anisotropy with the Young's modulus along several crystallographic directions being significantly higher (elastically stiff directions) than in along others (elastically soft directions).

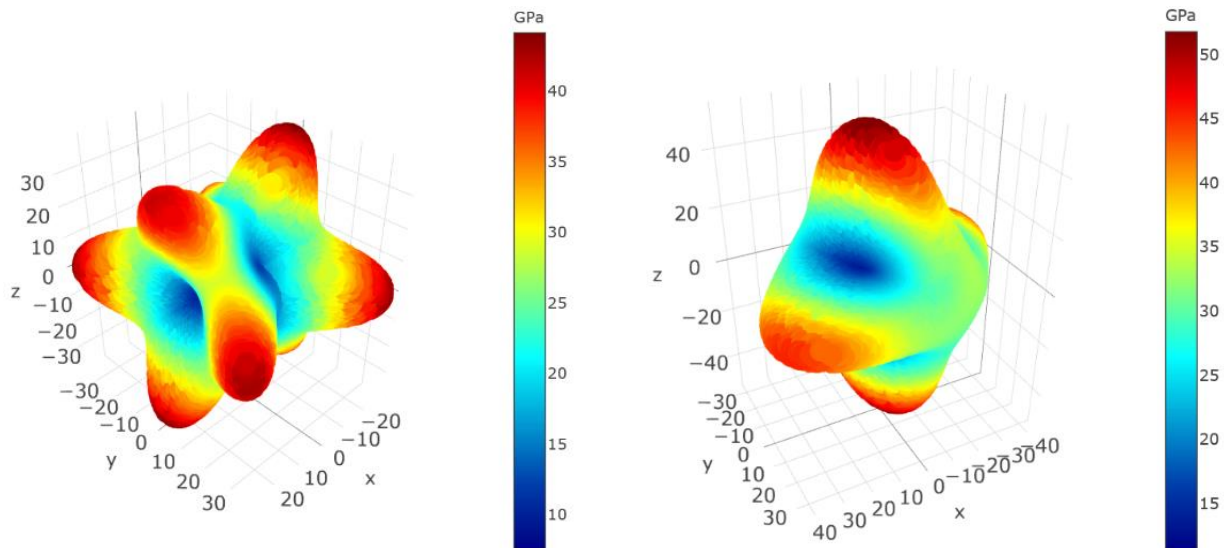


**Figure 4** Directional dependencies of single-crystal Young's moduli of the phases shown in Figures 2(c,d) (on the left) and in Figures 3(c,d) (on the right). The dependences are visualized by the MELASA software [22] (<https://melasa.cerit.sc.cz/>) using the computed single-crystal elastic constants.

We assume that the structures found in our calculations are very likely only local minima and the process of transformations and decomposition will continue. The apparent structural instability can be the reason why the initially published findings [6,8] could not be reproduced by the subsequent studies, e.g. Ref. [7], see also our paper [23].

#### 4. CONCLUSION

We have performed a quantum-mechanical study of Pb-supersaturated Pb-Sn solid solutions as materials associated with a decades-long controversy related to their crystal structure. We aimed at alloys with body-centred-tetragonal  $\beta$ -Sn structure and simple-hexagonal  $\gamma$ -Sn structure with a specific chemical composition  $\text{Pb}_5\text{Sn}_{11}$ , i.e. 31.25 at. % Pb, which is very close to the reported experimental value of 30 at. % Pb. In order to mimic an expected disorder in these alloys, the Pb atoms were distributed according to the special quasi-random structure (SQS) concept. We have performed so-called full structural relaxation of both  $\beta$ - and  $\gamma$ -phase alloys when the atomic positions, the supercell shape as well as its volume are changed to minimize the energy. The relaxations resulted in significant atomic re-arrangements providing unidentified structures that do not exhibit structural features typical for any allotrope of Pb-Sn alloys. The thermodynamic stability of the studied alloys (after the full relation) was assessed by computing the formation energies. The formation energies equal 50 meV/atom and 53 meV/atom for the  $\beta$ - and  $\gamma$ -phase-originating structure, respectively. The studied phases are, therefore, unstable with respect to the decomposition into the elemental lead and tin.

Further, we also computed the elastic constants of both phases, and our analysis of the values revealed that both phases are mechanically stable but close to mechanical instability. Our results indicate that the studied Pb-supersaturated Pb-Sn solid solutions may be prone to structural instability, transformations into different crystallographic phases and decomposition. Our findings can explain why subsequent experimental studies could not reproduce the preceding reported results.

## ACKNOWLEDGEMENTS

**M.F., P.Č., P.R., I.M., Š.M. and A.M. acknowledge the Czech Science Foundation for the financial support received under Project No. 22-05801S. Computational resources were provided by the e-INFRA CZ project (ID:90254), supported by the Ministry of Education, Youth and Sports of the Czech Republic. These resources were utilized through IT4Innovations National Supercomputing Center, MetaCentrum, and CERIT Scientific Cloud. Figures 1, 2 and 3 were visualized by the VESTA software [24].**

## REFERENCES

- [1] CHIAVARI, C., MARTINI, C., POLI, G., PRANDSTRALLER, D. Deterioration of tin-rich organ pipes. *Journal of Materials Science*. 2006, vol. 41, pp. 1819. Available from: <https://doi.org/10.1007/s10853-006-2896-0>.
- [2] ZHANG, L., TU, K.N. Structure and properties of lead-free solders bearing micro and nano particles. *Materials Science and Engineering: R: Reports*. 2014, vol. 82, pp. 1. Available from: <https://doi.org/10.1016/j.mser.2014.06.001>.
- [3] KARAKAYA, I., THOMPSON, W.T. The Pb–Sn (Lead-Tin) system. *Journal of Phase Equilibria (Bulletin of Alloy Phase Diagrams)*. 1988, vol. 9, pp. 144. Available from: <https://doi.org/10.1007/BF02890552>.
- [4] LEE, J.A., RAYNOR, G.V. The Lattice Spacings of Binary Tin-Rich Alloys. *Proceedings of the Physical Society. Section B*, 1954, vol. 67, pp. 737. Available from: <https://doi.org/10.1088/0370-1301/67/10/301>.
- [5] FRANKENTHAL, R.P., SICONOLFI, D.J. The equilibrium surface composition of tin-lead alloys. *Surface Science*, 1982, vol. 119, pp. 331. Available from: [https://doi.org/10.1016/0039-6028\(82\)90301-6](https://doi.org/10.1016/0039-6028(82)90301-6).
- [6] KANE, R.H., GIESSEN, B.C., GRANT, N.J. New metastable phases in binary tin alloy systems. *Acta Metallurgica*, 1966, vol. 14, pp. 605. Available from: [https://doi.org/10.1016/0001-6160\(66\)90068-X](https://doi.org/10.1016/0001-6160(66)90068-X).
- [7] SARODE, P.R., CHETAL, A.R. Metastable solid solutions in lead-tin alloys. *Current Sci*. 1974, vol. 43, pp. 339.
- [8] FECHT, H.J., ZHANG, M.X., CHANG, Y.A., PEREPEZKO, J.H. Metastable phase equilibria in the lead-tin alloy system: Part II. Thermodynamic modeling. *Metallurgical Transactions A*, 1989 vol. 20, pp. 785. Available from: <https://doi.org/10.1007/BF02651646>.
- [9] KRESSE, G., HAFNER, J. Ab initio molecular dynamics for liquid metals. *Physical Review B*, 1996, vol. 47, pp. 558. Available from: <https://doi.org/10.1103/PhysRevB.47.558>.
- [10] KRESSE, G., FURTHMÜLLER, J. Efficient iterative schemes for ab initio total energy calculations using a plane-wave basis set. *Physical Review B*, 1996, vol. 54, pp. 11169. Available from: <https://doi.org/10.1103/PhysRevB.54.11169>.
- [11] HOHENBERG, P., KOHN, W. Inhomogeneous electron gas. *Physical Review B*, 1964, vol. 136, pp. B864. Available from: <https://doi.org/10.1103/PhysRev.136.B864>.
- [12] KOHN, W., SHAM, L. J. Self-consistent equations including exchange and correlation effects. *Physical Review A*, 1965, vol. 140, pp. A1133. Available from: <https://doi.org/10.1103/PhysRev.140.A1133>.
- [13] BLÖCHL, P. E. Projector augmented-wave method. *Physical Review B*, 1994, vol. 50, pp. 17953. Available from: <https://doi.org/10.1103/PhysRevB.50.17953>.
- [14] KRESSE, G., JOUBERT, D. From ultrasoft pseudopotentials to the projector augmented-wave method. *Physical Review B*, 1999, vol. 59, pp. 1758. Available from: <https://doi.org/10.1103/PhysRevB.59.1758>.
- [15] PERDEW, J. P., BURKE, K., ERNZERHOF, M. Generalized gradient approximation made simple. *Physical Review Letters*, 1996, vol. 77, pp. 3865. Available from: <https://doi.org/10.1103/PhysRevLett.77.3865>.
- [16] FRIÁK, M., MASNIČÁK, N., SCHNEEWEISS, O., ROUPCOVÁ, P., MICHALCOVÁ, A., MSALLAMOVÁ, Š., ŠOB, M. Multi-methodological study of temperature trends in Mössbauer effect in Sn. *Computational Materials Science*, 2022, vol. 215, pp. 111780. Available from: <https://doi.org/10.1016/j.commatsci.2022.111780>.
- [17] ZUNGER, A., WEI, S., FERREIRA, L., BERNARD, J. Special quasirandom structures. *Physical Review Letters*, 1990, vol. 65, pp. 353. Available from: <https://doi.org/10.1103/PhysRevLett.65.353>.
- [18] OGANOV, A.R., GLASS, C.W. Crystal structure prediction using ab initio evolutionary techniques: Principles and applications. *The Journal of Chemical Physics*. 2006, vol. 124, pp. 244704. Available from: <https://doi.org/10.1063/1.2210932>.

- [19] LYAKHOV, A.O., OGANOV, A.R., STOKES, H.T. Zhu, Q. New Developments in Evolutionary Structure Prediction Algorithm USPEX. *Computer Physics Communications*. 2013, vol. 184, pp. 1172. Available from: <https://doi.org/10.1016/j.cpc.2012.12.009>.
- [20] OGANOV, A.R., LYAKHOV, A.O., VALLE, M. How evolutionary crystal structure prediction works - and why. *Accounts of Chemical Research*. 2011, vol. 44, pp. 227. Available from: <https://doi.org/10.1021/ar1001318>.
- [21] ZHOU, L., HOLEC, D., MAYRHOFER, P.H. Alloying-related trends from first principles: An application to the Ti-Al-X-N system. *Journal of Applied Physics*. 2013, vol. 113, pp. 113510. Available from: <https://doi.org/10.1063/1.4795590>.
- [22] FRIÁK, M., LAGO, D., KOUTNÁ, N., HOLEC, D., REBOK, T., ŠOB, M. Multi-phase ELASTic Aggregates (MELASA) software tool for modeling anisotropic elastic properties of lamellar composites. *Computer Physics Communications*. 2019, vol. 247, pp. 106863. Available from: <https://doi.org/10.1016/j.cpc.2019.106863>.
- [23] FRIÁK, M., ČÍPEK, P., PAVLŮ, J., ZOBAC, O., ROUPCOVÁ, P., MIHÁLIKOVÁ, I., HOLEC D., MSALLAMOVÁ, Š., MICHALCOVÁ, A. submitted in *Metall. Mater. Trans. A Phys. Metall. Mater. Sci.* (2023).
- [24] MOMMA, K., IZUMI, F. VESTA 3 for three-dimensional visualization of crystal, volumetric and morphology data. *Journal of Applied Crystallography*. 2011, vol. 44, pp. 1272. Available from: <https://doi.org/10.1107/S0021889811038970>.